

Characterization of the fatigue behavior of brazed steel joints by digital image correlation (DIC)

Michael Koster^{1,*}, Christoph Kenel¹, Christian Leinenbach¹

¹ Empa - Swiss Federal Laboratories for Materials Science and Technology; Laboratory for Joining Technologies and Corrosion; Überlandstrasse 129; 8600 Dübendorf; Switzerland

* Corresponding author: Michael.Koster@empa.ch

Abstract

In the actual work, the fatigue induced damage evolution in brazed steel joints - in particular under the influence of artificial brazing defects - was investigated using digital image correlation (DIC). The brazed joints consist of the soft martensitic stainless steel AISI CA 6-NM as substrate material and Au 18wt.-% Ni as a filler metal. Brazing was performed in a shielding gas furnace with an H₂ atmosphere. Besides the lifetime-oriented investigations, the cyclic deformation behavior was investigated using DIC. The measurements show that it is possible to monitor localized accumulating fatigue damage in an early state of the experiment. Besides the determination of the local strains, the deformation zones in the vicinity of strain concentrations could be characterized in detail. A high frequency camera allowed characterizing the damage evolution in the brazing zone during cyclic loading and investigating crack initiation and crack propagation during cyclic loading. The results are in correlation with SEM investigations and allow a more profound understanding of the failure mechanisms of brazed steel joints.

Keywords brazing, fatigue, defect, fracture, DIC

Nomenclature

Roman Symbols

a	[mm]	Defect size
A	[%]	Elongation at fracture
BSE	[--]	Back scattered electrons
d	[mm]	Thickness of the braze layer
DIC	[--]	Digital image correlation
E	[MPa]	Young's Modulus
N _f	[--]	Number of cycles to fracture
N _{max}	[--]	Maximum number of cycles
R	[--]	Load ratio
SEM	[--]	Scanning electron microscopy

Greek Symbols

σ_{UTS}	[MPa]	Ultimate tensile strength
σ_{max}	[MPa]	Maximum applied load for cyclic testing on the defect-free assumed cross section
σ_y	[MPa]	Yield strength

1. Introduction

Brazing has gained increasing importance as a favorable joining technology for many seminal applications in industry in the last years. Generally, brazing plays an essential role because the thermal stress of the joining partners and the processing times can be reduced, compared to e.g. welding. Furthermore, brazing allows joining of dissimilar materials as e.g. metals and ceramics at narrow tolerances. With the use of advanced brazing technologies, as e.g. high temperature (HT) vacuum furnace brazing, brazed joints can also be used for thermally and mechanically heavily loaded components in chemical engineering, power generation and for the production of power electronic components [1-3].

By definition, brazing is performed by heating an assembly over the melting point of the filler metal placed between two substrates without reaching the melting point of the substrate material. The liquid filler metal wets the surfaces of the substrate material and fills the joint gap. Subsequent adhesion and diffusion processes during the cooling of the assembly are essential for the final joint strength. The general differentiation between soldering and brazing is made according to the process temperatures used for the joining process. The above described process at $T < 450$ °C is referred to as soldering, whereas it is named brazing at $T > 450$ °C.

Generally, brazed joints form heterogeneous systems, consisting of base material, filler metal and diffusion zone. Under mechanical loading, the properties of brazed joints vary significantly from those of the individual joining partners. The complex deformation behavior of the brazed joint is characterized by geometrical and microstructural interactions as e.g. by different elastic-plastic properties of substrate material and thin braze layer. Uniaxial loading and the constrained deformation of the thin filler alloy layer can lead to a triaxial stress state which strongly influences the joint performance [4]. To estimate the influence of defects on bulk materials and on welded structures under quasi-static loadings, defect assessment procedures, such as R6, BS7910 or SINTAP have been developed [5 - 8]. In the scope of previous investigations [9], it has been shown that the R6-procedure can also be used to estimate the influence of defects on brazed joints. In previous studies, a rather unusual fatigue crack growth behavior of brazed steel joints, i.e. extremely steep $da/dN-\Delta K$ curves in comparison with the ones of bulk materials, was observed [4]. It could be shown that under defined boundary conditions, the influence of defects on the fatigue lifetime can be estimated based on the stress intensity factor caused by the defect [10], but up to date information on the general influence of brazing defects on the fatigue behavior of brazed joints is lacking. Therefore, a better understanding of fatigue crack initiation and propagation is very important for reliable life-time predictions of brazed joints.

Generally, during stress-controlled fatigue tests with metallic materials, fatigue is closely related to the evolution of (local) irreversible strains. In homogenous materials, the strains are relatively equally distributed over a macroscopic length scale and can therefore be averaged using integrating measurement techniques, e.g. with extensometers. However, plastic strains in brazed joints are usually localized in a small volume in or next to the brazing zone. The thickness of braze layers is usually in the range of 50-100 μm , so conventional strain measuring techniques cannot be applied reasonably. To measure local strains during cyclic loading with a sufficiently high resolution, digital image correlations (DIC) were performed. The technique was applied to monitor the fatigue induced damage evolution in brazed steel joints during cyclic loading, in particular under the influence of brazing defects. Furthermore, the fracture surfaces were analyzed by SEM to correlate the experimental results with characteristic deformation features and to obtain information on the underlying failure mechanisms.

2. Testing materials and experimental setup

The brazed joints used for the actual investigations consisted of the steel AISI CA 6-NM (X 3 CrNiMo 13-4) as substrate material and of the gold-nickel alloy Au-18wt.-% Ni as filler metal. The substrate material contains 0.05 wt.-% carbon, 13wt.-% chromium, 4 wt.-% nickel and small amounts of molybdenum. Brazing was performed using foils of the filler metal with a thickness of $d = 100 \mu\text{m}$. Besides its comparably low melting point of 955°C , the filler metal is characterized by good corrosion resistance and excellent wetting behavior. The brazing process was performed at $T \approx 1000^\circ\text{C}$ in reducing atmosphere with H_2 as a shielding gas. After brazing, a two-step heat treatment procedure was performed at $T_1 \approx 700^\circ\text{C}$ and $T_2 \approx 650^\circ\text{C}$ with N_2 as a shielding gas to optimize the mechanical properties of the brazed joints and to improve the materials resistance against stress corrosion cracking. The mechanical properties of the substrate material, filler metal and brazed joints taken from round specimens are shown in Table 1. The mechanical properties of the filler metal were measured in the scope of in situ SEM investigations [9].

Table 1: Mechanical properties of base material, filler metal and brazed joint

	E [GPa]	σ_y [MPa]	σ_{UTS} [MPa]	A [%]	HV0.05
AISI CA 6-NM	203	726	844	20.0	327
Au-18wt.-%Ni	110	555	940	6.5	271
Brazed, round	200	721	841	10.3	--

Further tensile tests were performed with T-joint specimens. Due to their specimen geometry, conventional strain measurements with an extensometer were not applicable. The experiments show that the σ_{UTS} of brazed T-joints without defects averages 835 MPa.

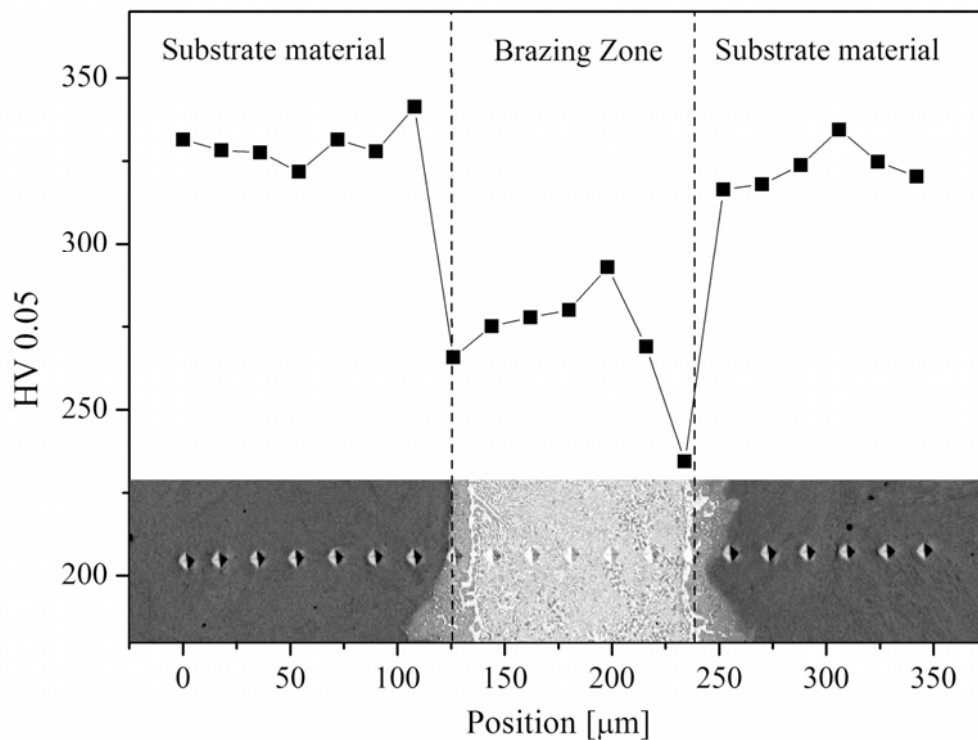


Figure 1: Microstructure and hardness measurements of a brazed joint

As shown in the BSE-micrograph in Figure 1, the joint consists of base material, filler metal and diffusion zone.

In the brazing zone, the filler metal consists of a gold-rich phase and an iron-nickel-rich phase whereas in the region between substrate material and braze layer, the penetration of gold into the substrate material was observed, as is also reported in the literature [11]. Adjacent to the diffusion zone, a layer of the precipitate-free gold-rich phase is formed, that provides the lowest hardness values of 235 HV 0.05.

For the actual experiments T-joints with and without artificial brazing defects were investigated. T-joints are characterized by a sudden change of the cross section area at the brazing zone, as shown in Figure 2. They were designed with respect to the original geometry of a turbo compressor impeller.

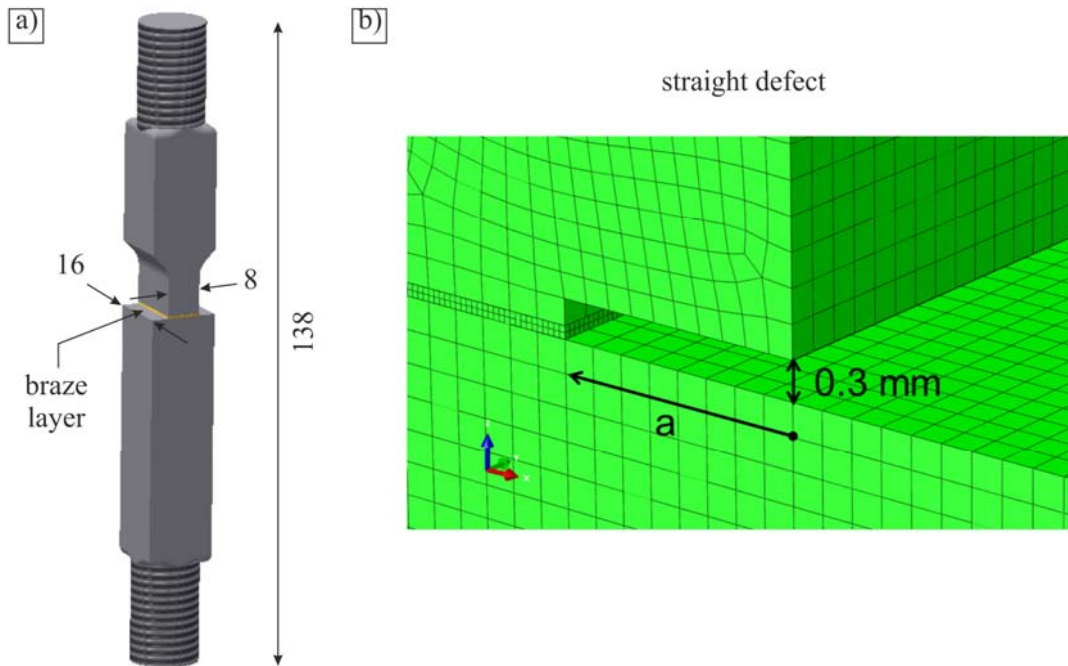


Figure 2: a) Geometry of the T-joint specimen and b) defects introduced into the braze layer

To simulate typical brazing defects like partly unfilled brazing gaps or large pores, straight defects with sizes of $a = 0.5$ mm, $a = 1$ mm and $a = 2$ mm (cf. Fig. 2b) were introduced into the braze layer by electrical discharge machining.

The stress-controlled cyclic loading experiments were performed on a servo-hydraulic testing machine at a frequency of 5 Hz. To simulate the influence of start/stop cycles, the experiments were performed at a load ratio of $R = 0.1$ until $N_{\max} = 2 \cdot 10^4$ cycles. Besides the lifetime oriented investigation of the fatigue behavior, event-oriented experiments were performed with DIC.

The DIC analysis was performed with a black speckle pattern on a white coating on the side surfaces of the T-specimens. To guarantee a sufficient resolution of the object displacements, the pattern was prepared with an average speckle size of 35 μm . The spray painting system used was an airbrush device with a nozzle diameter of 0.2 mm and gravity feed. The image acquisition was performed with a high speed camera (Redlake MotionExtra HG100K) that was focused on the brazing zone. Series of pictures were taken at a recording speed of 500 fps and an aperture time of 500 μs . The DIC was performed with the software Moiree Analysis V0.950[©] by correlating images of the maximum and the minimum force at defined loading cycles. The use of a high frequency camera allows investigating the development of strains during cyclic loading. Especially for brazed specimen, as a typical representative for heterogeneous systems, this technique allows to study the crack initiation, the crack propagation and the influence of stress concentrations as e.g. defects

locally with an adequate lateral and temporal resolution.

After the experiments, SEM investigations were performed to analyze the fracture surface and to correlate the results with DIC. To distinguish between volumes with different chemical compositions, a BSE detector was chosen for the investigations. Therefore, volumes containing heavy elements as gold are shown in bright contrast whereas comparably light elements are shown in dark contrast.

3. Results

Figure 1 shows the maximum applied loading amplitude of the defect-free assumed cross section as a function of the numbers of cycles to failure.

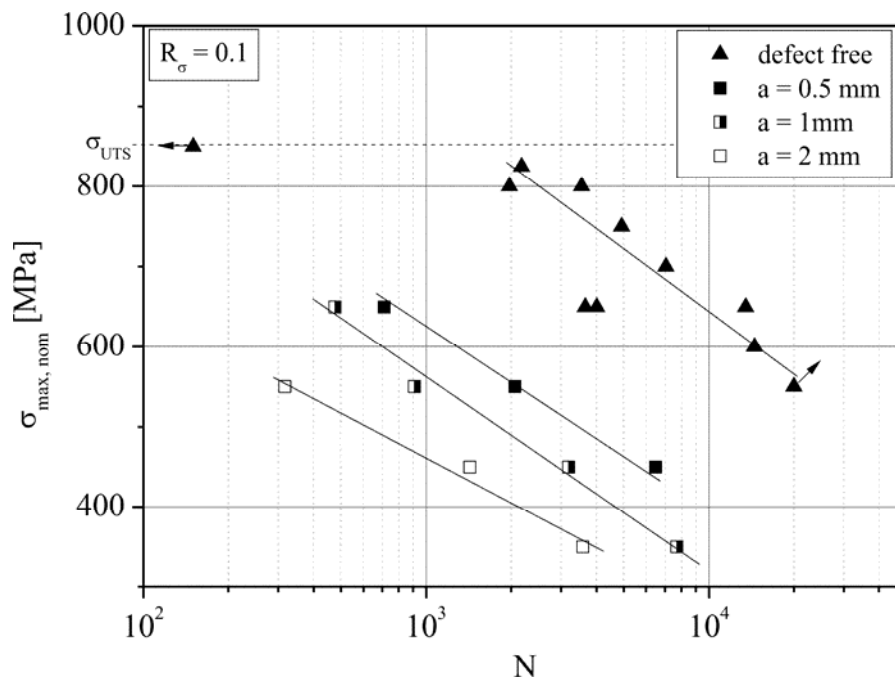


Figure 3: S,N curve of defect-free and defect containing T-joint specimens

The results of the experiments show that defects significantly influence the joint strength. As could be expected, defects lead to a decrease of the joint strength. The larger the defect, the more pronounced the decrease of the fatigue strength. Defect-free specimens can be loaded even up to the ultimate tensile strength of the substrate material for 50 loading cycles, as shown in Figure 3. This can be explained by the ductile deformation and hardening behavior of the substrate material. Loadings around the yield strength of the material lead to failure of the defect-free specimens at approx. 10^4 loading cycles. S,N-curves can be used to describe the influence of one defined defect, but they are not suitable to describe the influence of defects varying in form, shape and position reasonably. In a previous study, a fracture mechanical approach to estimate the influence of brazing defects on a universal scale is based on the stress intensity caused by a defect was successfully applied to make life-time predictions for joints of a less ductile steel [10]. However, this approach did not lead to reasonable results for the material used in this work.

The local strain evolution was characterized experimentally by DIC. Figure 6 shows a defect-free specimen at several stages during cyclic loading at $\sigma_{max} = 650$ MPa until $N_f = 13518$ cycles. The strain distribution in the first and in the loading cycle before failure occurred is shown in Figure 4 together with the speckle in the background.

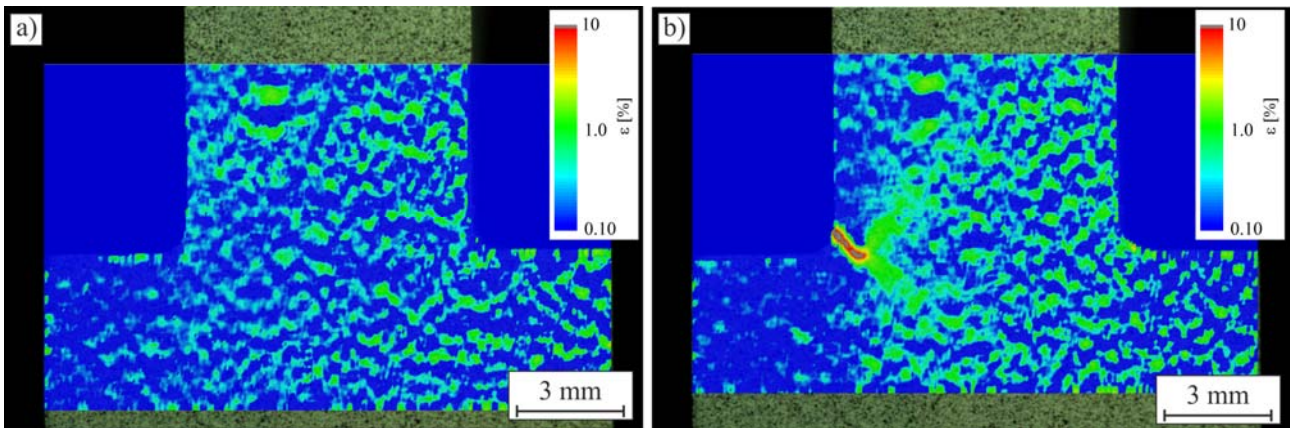


Figure 4: DIC with a defect free specimen

During the first loading cycles, the strains are equally distributed over the whole cross section (Figure 4 a). During further cycling, the fatigue damage accumulation leads to increased local strains and subsequent crack initiation and propagation. Figure 4b shows the deformations in the last cycle before fracture. Furthermore, Figure 4b shows that the crack initiates in the fillet, not directly in the braze layer, as could be expected. Then, it grows at an angle of approximately 45° to the loading direction until it changes its direction and propagates in the vicinity of the brazing zone, perpendicular to the loading direction.

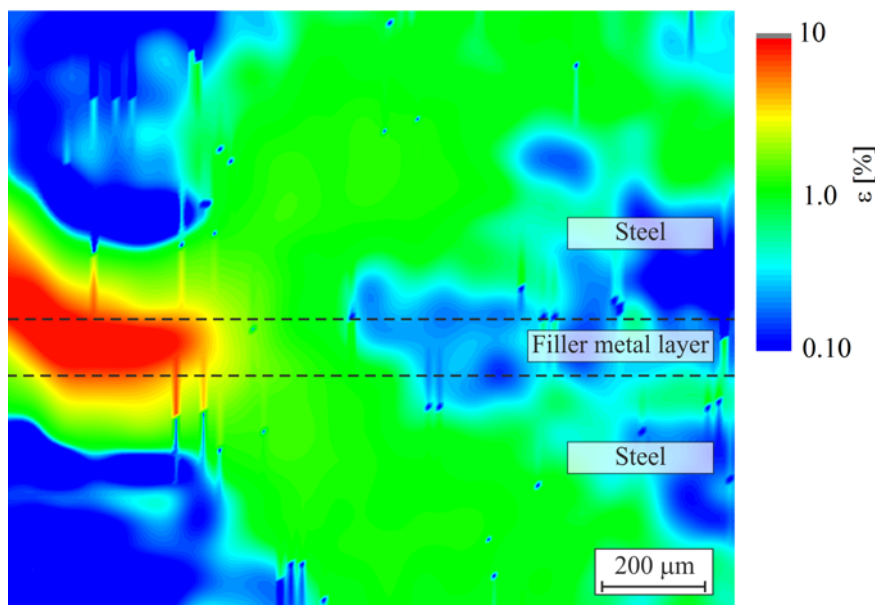


Figure 5: DIC – Strain field in the vicinity of the fatigue crack

Figure 5 shows a close-up image correlation of the crack tip region, the approximate position of the filler metal layer is indicated by dashed lines. Whereas the highest strains are found at the position of the crack due to the crack opening, the volume ahead of the crack tip exhibits also increased strains. With increasing distance these high strains are located in wing-shaped strain fields in the parent material. The filler metal is only subjected to a strain level comparable to the wing-shaped strain fields in a region of 300 μm ahead of the crack tip, whereas in further distance the enhanced stress levels are only observed in the parent material. Some of the data points shown in blue represent regions where no correspondence was found. The strain interpolation with the neighboring values leads to the vertical stripes in Figure 5.

A further experiment was performed with a defect containing specimen with $a = 1$ mm that was subjected to $\sigma_{\max} = 350$ MPa. Failure occurred after $N_f = 7711$ loading cycles.

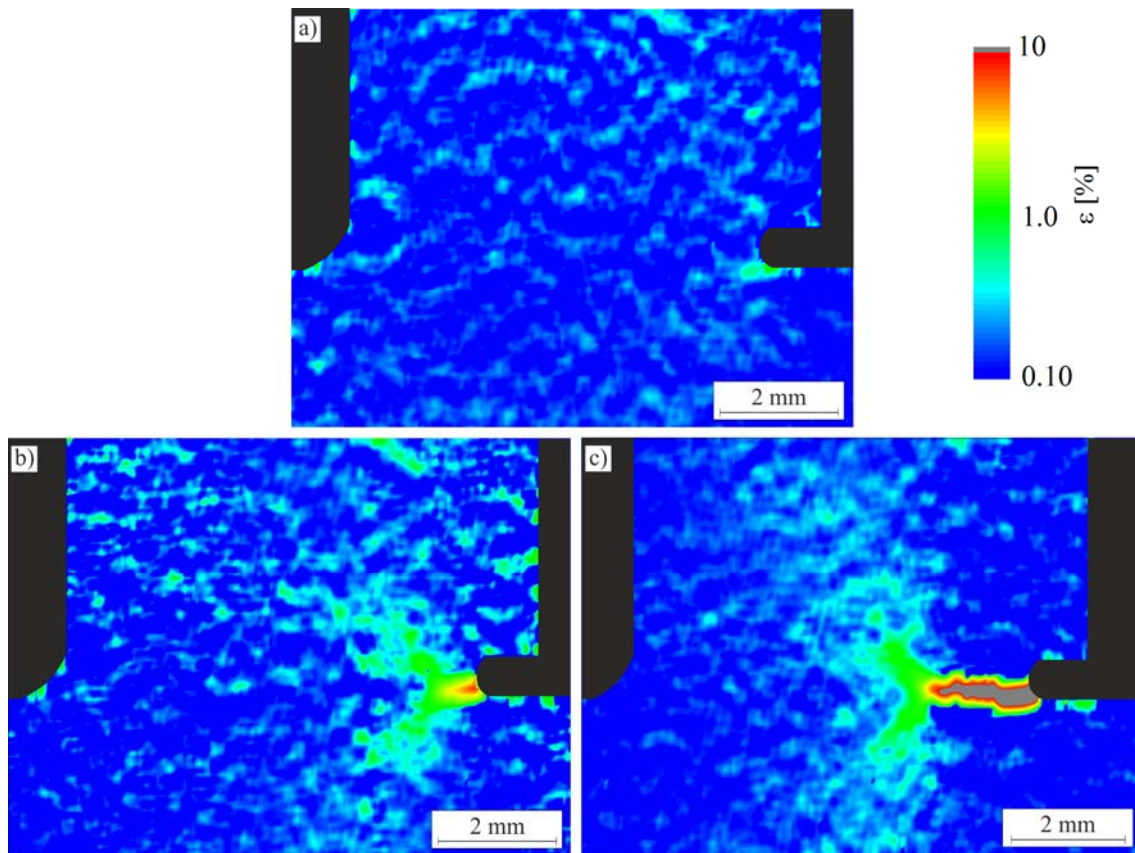


Figure 6: DIC of a defect containing specimen at a) $N = 100$ b) $N = 0.8 \cdot N_f$ and c) $N = N_f - 20$

The results of the DIC show the inhomogeneous distribution of local strains due to increased stresses at the tip of the defect already in an early state of the experiment. After 100 loading cycles, a slight increase of the strains can be measured at the tip of the defect (Figure 6a). At $N \approx 6200$ loading cycles ($\approx 0.8 \cdot N_f$), severe deformations indicate increasing strains as a result of accumulated fatigue damage at the approximate position of the braze layer at the tip of the defect (Figure 6b). Further cycling leads to crack initiation and crack growth. Figure 6c shows the local deformations 20 loading cycles before failure occurred. Due to the lacking possibility of differentiating between crack opening and a black speckle, the results in the direct proximity of the crack should be considered only qualitatively. Especially the volume ahead of the crack exhibits high strains that are distributed over a relatively large volume compared to the layer thickness of $d = 100$ μm . The wing shaped strain field that expands over 1 mm in front of the crack tip corresponds also to the strain field that has been determined for the defect free specimen (Figure 4b).

To investigate the mechanisms of crack growth, SEM investigations were performed on the fracture surfaces of the specimens shown in Figure 4 and Figure 6.

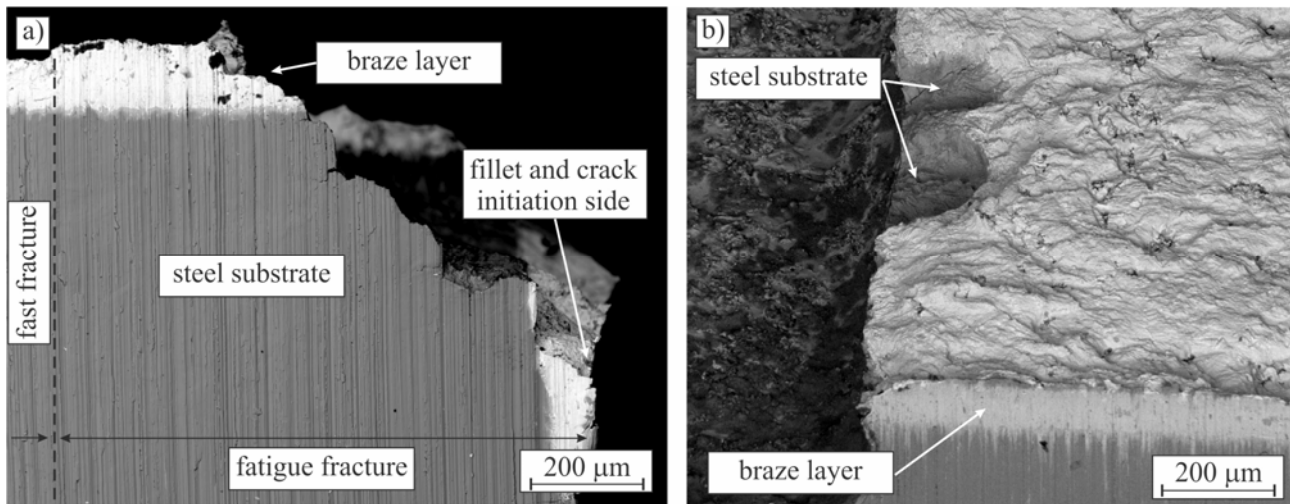


Figure 7: SEM investigations of the fracture surface for a) defect-free and b) defect containing T-joint

The SEM analysis correlates with the DIC calculations considering crack initiation and crack growth. Figure 7a shows the crack initiation side in the fillet and its growth at an angle of 45°, as was also shown in Figure 4b. The crack path through the substrate material is characterized by a discontinuous course. This could be an indicator for inter-crystalline crack growth that could result from the diffusion of liquid gold into the steel substrate between the grain boundaries, as described in [11]. Next to the main crack, multiple secondary cracks were found in the substrate material and in the braze layer. The crack growth follows the same direction until it has passed the braze layer and reached the opposite interface. There, it changes direction and follows the interfacial zone until it has reached a critical length and fast fracture occurs. The fracture surface of the defect containing specimen is shown in Figure 7b. Also for this specimen, the crack passes through the substrate material.

Conclusions

The results show that defects in the brazing zone strongly influence the fatigue lifetime of brazed components. It could be shown that DIC allows measuring local displacements during cyclic loading with a sufficiently high resolution. Continuing fatigue damage is indicated before final failure occurs by increasing strains around structural hot spots. Wing shaped strain fields in front of the crack tip extend over a comparable large volume of the substrate material. Furthermore, the results allow to draw conclusions on the mechanisms of crack initiation and to monitor crack growth during cyclic loading, which is important for braze joints. The results of the DIC show that for defect-free and for the defect containing T-joint specimen, the crack does not necessarily follow the softer filler metal but propagates through both the substrate material and the braze layer. Only when the crack reaches the opposite interface of the braze layer it changes its direction and follows the interfacial regions on its path. Further experiments will be performed to characterize the fatigue behavior of brazed joints with special interest on the influence of defects. In the future, DIC will be performed to investigate the fatigue crack growth behavior more precisely. In correlation with SEM investigations, the presented methods can be used to achieve a better understanding of the mechanisms that lead to failure of brazed steel joints.

Acknowledgement

The authors gratefully thank MAN Diesel & Turbo AG Zürich for financing this project

References

- [1] T. Ma, M. Zeng, Y. Ji, H. Zhu, Q. Wang, Investigation of a novel bayonet tube high temperature heat exchanger with inner and outer fins. *Int. J. Hydrogen Energy*, 36 (2011) 3757-3768.
- [2] J. Novacki, P. Swider, Producibility of brazed High-dimension Centrifugal Compressor Impellers. *J. Mater. Process. Technol.*, 133 (2003) 174-180.
- [3] L. Sáncheza, D. Carrillo, E. Rodrígueza, F. Aragóna, J. Sotelob, F. Torala, Development of high precision joints in particle accelerator components performed by vacuum brazing. *J. Mater. Process. Technol.*, 211 (2011) 1379-1385.
- [4] C. Leinenbach, H.-J. Schindler, Mechanics of fatigue crack growth in a bonding interface. *Eng. Fract. Mech.*, 89 (2012) 52-64.
- [5] Y.J. Kim, M. Koçak, R.A. Ainsworth, U. Zerbst, SINTAP defect assessment procedure for strength mismatched structures. *Eng. Fract. Mech.*, 67 (2000) 529-546.
- [6] British Energy Generation Ltd., Assessment of the integrity of structures containing defects. R6-Rev. 4 (2002).
- [7] British Standard, Guide on methods for assessing the acceptability of flaws in metallic structures. BS 7910 (1999).
- [8] S. Webster, A. Bannister, Structural integrity assessment procedure for Europe – of the SINTAP programme overview. *Eng. Fract. Mech.*, 67 (2000) 481-514.
- [9] C. Leinenbach, H.-J. Schindler, T.A. Başer, N. Rüttimann, K. Wegener, Quasistatic fracture behaviour and defect assessment of brazed soft martensitic stainless steel joints. *Eng. Failure Anal.*, 17 (2010) 672-682.
- [10] C. Leinenbach, M. Koster, H.-J. Schindler, Fatigue assessment of defect-free and defect containing brazed steel joints. *J. Mater. Eng. Perform.*, 5 (2012) 739-747.
- [11] D. Favez, L. Deillon, J.-D. Wagnière, M. Rappaz, Intergranular penetration of liquid gold into stainless steel. *Acta Mater.*, 59 (2011) 6530-6537.